Inhibitory actions of the selective serotonin re-uptake inhibitor citalopram on HERG and ventricular L-type calcium currents

Harry J. Witchel[a,*], Vijay K. Pabbathi[a], Giovanna Hofmann[b,1], Ashok A. Paul[a], Jules C. Hancox[a]

[a] *Cardiovascular Research Laboratories and Department of Physiology, School of Medical Sciences, University Walk, Bristol BS8 1TD, UK*
[b] *International School for Advanced Studies (SISSA), INFM Unit, Via Beirut 2–4, 34014 Trieste, Italy*

Received 29 November 2001; accepted 7 December 2001

First published online 4 January 2002

Edited by Maurice Montal

Abstract **Using whole-cell patch clamp recording of heterologous HERG-mediated currents in transfected mammalian cells, we observed that the selective serotonin re-uptake inhibitor citalopram blocks HERG with an IC_{50} of 3.97 μM. This is slightly less potent than fluoxetine in our system (IC_{50} of 1.50 μM). In isolated guinea pig ventricular cardiomyocytes citalopram inhibited L-type calcium current ($I_{Ca,L}$). The voltage dependence of $I_{Ca,L}$ inactivation in the presence of 100 μM citalopram was shifted significantly leftward. As a result, the $I_{Ca,L}$ 'window' in citalopram was found to be (a) smaller and (b) leftward-shifted compared to control. The effects of citalopram on both calcium current amplitude and the $I_{Ca,L}$ 'window' may help to explain citalopram's good cardiac safety profile, given its propensity to block HERG at excessive dosages.**

Key words: Acquired long QT syndrome; Citalopram; Early afterdepolarisation; Fluoxetine; HERG; $I_{Ca,L}$; I_{Kr}; Myocyte; Rapid delayed rectifier; Selective serotonin re-uptake inhibitor; SSRI

1. Introduction

In cases of self-poisoning by a single agent, tricyclic antidepressants (TCAs) are associated with higher fatal toxicity indices than are selective serotonin re-uptake inhibitors (SSRIs), and this is presumably due to QT prolongation of the electrocardiogram (ECG) and the associated arrhythmogenesis that can accompany TCA overdose [1–4]. Within the clinical concentration range, TCA use, but not SSRI use, is a significant risk factor for lengthening of the QT interval of the ECG in psychiatric patients [5], and SSRIs are thought to be safer than TCAs in the background of cardiovascular risk [6]. Citalopram is an SSRI that has similar efficacy against depression to other SSRIs, and to tetracyclic antidepressants and TCAs [7]. In contrast to TCAs, citalopram is reputed to have a good safety profile at concentrations within the clinical range [7,8]; therefore, citalopram may be an attractive agent for treatment of patients who cannot tolerate the cardiovascular adverse effects of TCAs or who suffer comorbid illness that also requires drug treatment. However, considerable controversy has arisen over the possible effects of citalopram in overdose, particularly with regard to QT prolongation and potential arrhythmogenic risk [9–13].

The risk of QT prolongation and associated arrhythmia by TCAs corresponds at the cellular level with pharmacological inhibition of native cardiac delayed rectifier potassium (K^+) channels [14] and current carried by the cloned α subunit mediating the rapid delayed rectifier current – HERG [15]. TCAs such as imipramine and amitriptyline inhibit HERG channels at clinically relevant concentrations [16–18]. The actions of SSRIs such as citalopram on HERG channels have not yet been reported. The reported safety profile of the agent might lead to a prediction that HERG channels are insensitive to citalopram. The aim of the present study was to test this experimentally, using heterologously expressed HERG K^+ channels. We report here that HERG is sensitive to inhibition by citalopram. However, we also found that this drug can inhibit cardiac L-type calcium (Ca^{2+}) current ($I_{Ca,L}$), and it is possible that this effect may offset QT prolongation and the associated pro-arrhythmia that would otherwise occur as a result of selective HERG blockade.

2. Materials and methods

2.1. Transient expression of HERG

The transient expression of HERG was performed using Chinese hamster ovary (CHO) cells that were maintained as described previously [19]. In brief, cDNA encoding the HERG channel subunit was subcloned into pGW1H, which contains a CMV promoter to drive expression of the insert. Cells were plated onto small sterilised glass coverslips and after 24 h the cells were co-transfected with 3:1 HERG cDNA:green fluorescent protein (GFP) in pCMX using the recommended lipofectamine (BRL) protocol. Cells were washed with Optimem (BRL) medium, and after a 45 min incubation together, a mixture including 6 μl lipofectamine solution with 1 μg total plasmid DNA was added to cells in a 30 mm petri dish, followed by a 4 h incubation before the reintroduction of 10% (final) foetal bovine serum. Between 20 and 36 h after transfection coverslips were transferred to the recording chamber. Additional measurements were made from a human embryonic kidney cell line (HEK 293) stably expressing

*Corresponding author. Fax: (44)-117-928 8923.
E-mail address: harry.witchel@bris.ac.uk (H.J. Witchel).

[1] Present address: Department of Experimental Pathology and Oncology, Institute of General Pathology, University of Florence, Viale G.B. Morgagni 50, 50134 Florence, Italy.

Abbreviations: ECG, electrocardiogram; EAD, early afterdepolarisation; HERG, human ether-a-go-go related gene; $I_{Ca,L}$, L-type calcium current; SSRI, selective serotonin re-uptake inhibitor; TCA, tricyclic antidepressant

0014-5793/02/$22.00
PII: S0014-5793(01)03320-8

HERG and maintained as previously described [20]; some small differences in the recording conditions (described below) of the two types of cells were made, which led to increased cell longevity during recording for each type of cell. No statistical difference between citalopram blockade of HERG (tail current maximum at −40 mV) in the two heterologous systems in the two sets of recording conditions was observed at the two concentrations tested (3 μM and 100 μM; unpaired *t*-test, $P > 0.2$ for both, $n = 3$–8).

2.2. Guinea pig isolated ventricular myocytes

Myocytes were isolated from both ventricles of male guinea pig (~400 g) hearts, using an enzymatic dispersion method described previously [21]. The cells were stored at room temperature in solution containing 1 mM Ca^{2+} until required for use. Cells remained viable for up to 8 h after isolation.

2.3. Electrophysiological recording

2.3.1. HERG current (I_{HERG}) measurement in transiently transfected cells. Whole-cell patch clamp recordings were made at 20°C in normal Tyrode's solution containing (in mM): 140 NaCl, 4 KCl, 2 $CaCl_2$, 1 $MgCl_2$, 10 glucose, 5 HEPES (titrated to a pH of 7.4 with NaOH). Citalopram (Lundbeck) was added to this solution to the final concentrations mentioned in the text from a 30 mM stock solution made daily in de-ionised (Milli-Q) water. Patch pipettes (1.5 mm o.d. soda glass; Harvard Apparatus) were pulled to resistances of 4–5 MΩ. The K-based internal dialysis solution contained (in mM): 144 KCl, 8 Na_2HPO_4, 2 NaH_2PO_4, 1 Na_2ATP, 0.3 Na_2GTP, 2 $MgCl_2$, 0.5 EGTA (pH to 7.3 with KOH).

Membrane current recordings were made using List EPC-7 patch clamp amplifiers (Heka Elektronik). Current and voltage were sampled at rates between 1 and 20 kHz using a standard laboratory

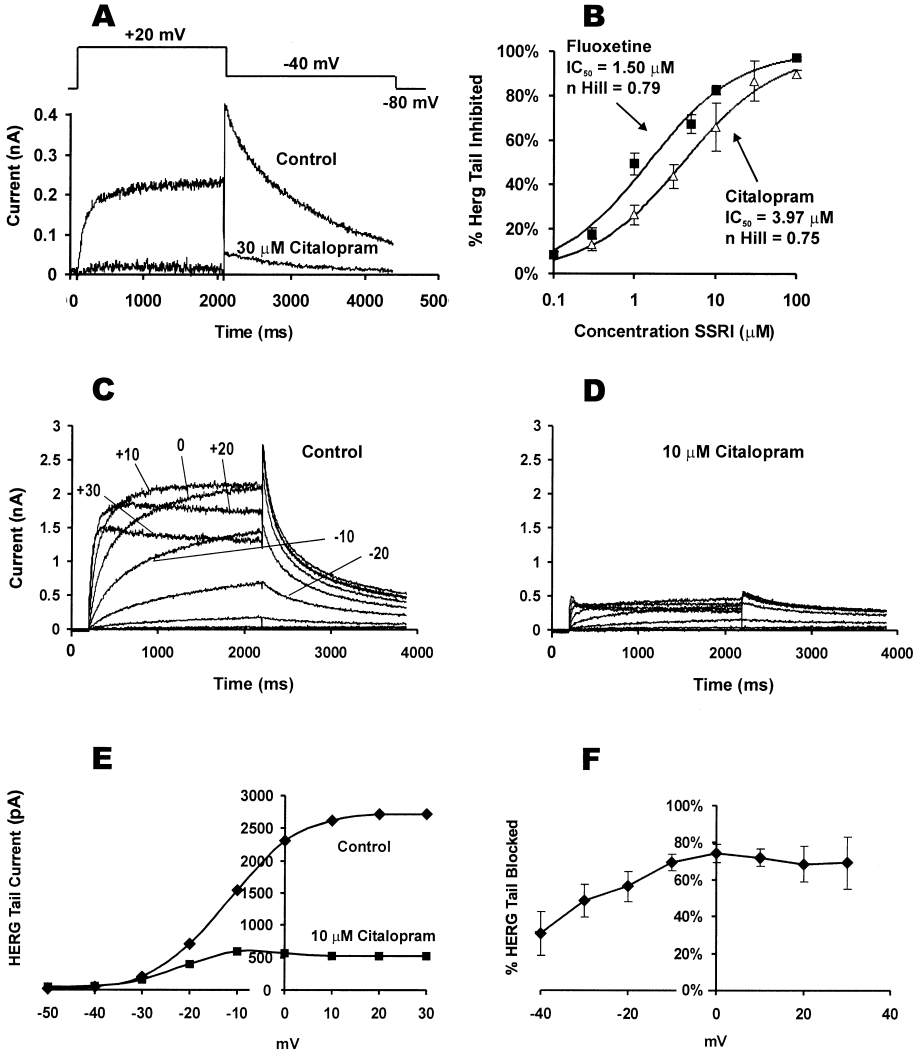

Fig. 1. Citalopram blocks HERG-mediated current. (A) shows representative current records from a cell before and after addition of 30 μM citalopram. After stable control recordings (hold −80 mV, step to +20 mV for 2 s, observe tail currents at −40 mV, a schematic of the voltage protocol is shown at the top of (A)) were attained, citalopram was superfused onto the cell for 2 min while the cell was held at −80 mV. Then the above protocol was repeated until blockade reached steady-state. (B) shows the means ± S.E.M. of a series of the same experiment, in which different concentrations of either citalopram (open triangles) or fluoxetine (closed squares) were applied to the cell. These were then fitted to a logistic equation. (C–F) show the voltage dependence of citalopram blockade of I_{HERG}. Cells expressing heterologous HERG were held at −80 mV and stepped to different voltages (−50 mV to +30 mV, 10 mV steps) for 2 s, and then tail currents were measured at −40 mV for 4 s ('IV protocol'; minimum 10 s interpulse interval). The cells were then allowed to equilibrate with 10 μM citalopram for 3–5 min while held at −80 mV. The cells were then stepped repeatedly to +20 mV (using the protocol in (A)) in the presence of citalopram until blockade reached equilibrium, after which the cells were subjected to the IV protocol again. (C) and (D) are examples of typical current records from one cell, control (C), 10 μM citalopram (D). Some of the individual traces in (C) are labelled with their depolarising test potentials (in mV) for clarity. (E) shows the IV relation for the peak tail currents (I_{HERG}) recorded during the step to −40 mV for the same representative cell. In (F) the average percentage of I_{HERG} blockade was calculated by subtracting the ratio of current with and without citalopram at a single voltage from unity for each cell before calculating the mean for all cells. $n = 5$.

interface (1401Plus, Cambridge Electronic Design) controlled by customised software [22]. Normally 75–80% of the electrode series resistance could be compensated.

2.3.2. I_{HERG} measurement in stably transfected cells. Methodologies and protocols for the stable cell line were identical to those of the transiently transfected cells with the following changes. Pipette glass used was Corning 7052 glass (AM Systems Inc.), and these were initially pulled to resistances of 2–3 MΩ and then fire-polished to 4–5 MΩ. Recordings were made at 35–37°C using a K-based internal dialysis solution containing (in mM): 110 KCl, 5 K_2ATP, 0.4 $MgCl_2$, 5 EGTA, 10 HEPES (titrated to pH 7.1 by adding KOH). The amplifier used was an Axopatch 1D amplifier (Axon Instruments) with a CV-4 1/100 headstage. Voltage clamp commands were generated using 'WinWCP', a program written and supplied free of charge by John Dempster (Strathclyde University) and data were recorded via a Digidata interface. The HERG-expressing HEK 293 stable cell line provided essentially identical results to the HERG transiently transfected CHO cells (see above).

2.3.3. $I_{Ca,L}$ measurement. A Cs^+-based internal dialysis solution was used for all $I_{Ca,L}$ recordings; its composition was as follows (in mM): 113 CsCl, 5 K_2ATP, 0.4 $MgCl_2$, 2 K_2EGTA, 5 glucose, 10 HEPES, titrated to pH 7.2 with CsOH. Isolated myocytes were bathed in a normal Tyrode's solution at 35–37°C until whole-cell clamp had been obtained, after which 'control' solution was applied (standard Tyrode's solution, free of external K^+, in order to inhibit inwardly rectifying K^+ current). Citalopram was added to this solution to the final concentrations mentioned in the text from a stock solution as described above. An Axopatch 200B amplifier, with a CV 202A headstage was used for all $I_{Ca,L}$ recordings. Pulse protocols were generated and membrane currents recorded using pCLAMP 7.0.

2.4. Data analysis and presentation

Data were analysed offline, using WinWCP, pCLAMP (Clampfit), Excel 5.0 and 'FigP for Windows' (Biosoft). Data are presented as mean ± S.E.M. and statistical comparisons were made using a paired Student's *t*-test (Systat, Systat Inc.). *P* values of <0.05 were taken as significant.

3. Results

3.1. Effects of citalopram on I_{HERG}

The effects of citalopram upon outward current associated with expression of the HERG transcript in mammalian cells were tested, without pharmacological inhibitors in either the external or pipette solutions, in the whole-cell mode of patch clamp. These cells have previously been shown to lack I_{HERG} when untransfected [16,20]. The membrane potential was held at −80 mV, and interpulse intervals were a minimum of 6 s to allow complete deactivation of the channel to occur between sweeps. To test the effect of citalopram on I_{HERG}, a 2 s step to +20 mV was used to activate (and inactivate) the current, and then tail currents were measured at −40 mV to allow for rapid recovery from inactivation; the peak of the tail current (I_{HERG}) was compared in the presence and absence of different concentrations of citalopram. In Fig. 1A a representative experiment comparing the current in normal Tyrode's solution (control) and in the presence of 30 μM citalopram is shown; the block was profound, with 86.6 ± 5.1% of I_{HERG} being blocked at this concentration ($n=7$); this concentration is well above the maximum plasma concentration of 120 ng/ml (nominally a maximum of 300 nM, ignoring drug binding) observed at the therapeutic dosages [8], but it may occur in cases of self-poisoning.

A series of citalopram concentrations were compared to control in order to determine the concentration response relationship for citalopram blockade of I_{HERG}, and this is shown in Fig. 1B. At 100 μM, the highest concentration attempted, I_{HERG} was blocked 90.0 ± 1.8% ($n=9$), and the data were fit-

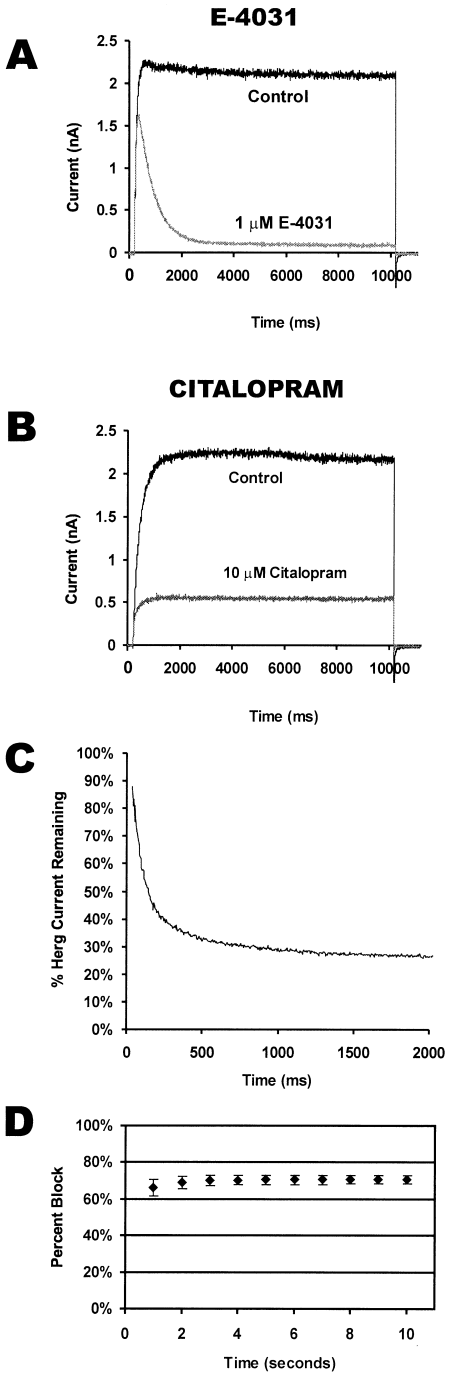

Fig. 2. Time dependence of citalopram blockade of I_{HERG}. Cells expressing heterologous HERG were held at −80 mV and stepped to 0 mV for 10 s. The cells were then allowed to equilibrate with either 1 μM E-4031 or 10 μM citalopram for 3–5 min while being held at −80 mV. The cells were then subjected to the same command protocol again. (A) shows a representative current record in the presence and absence of E-4031. (B–D) show experiments using 10 μM citalopram. (B) is a representative set of traces, and (C) shows the percentage I_{HERG} remaining (i.e. the ratio of current to current without citalopram) at each time point, and then the mean calculated for five cells during the first 2 s of the long pulse protocol. (D) shows that the block does not change after 3 s; for each cell at each 1 s interval a mean of current measured over 20 ms is calculated in the presence and absence of citalopram, and the percentage block for that time point is then calculated. The graph shows the means for five cells of the percentage block.

ted by computer to a logistic equation. The observed IC_{50} was 3.97 μM, and the Hill coefficient was 0.75 ($n = 5$–10 for all concentrations); this Hill coefficient may suggest that there was a one-to-one interaction between drug molecule and channel. This potency of I_{HERG} block is not dissimilar from that observed in our experimental system when testing the TCA imipramine: $IC_{50} = 3.4$ μM and $n_{Hill} = 1.17$ [16].

3.2. Fluoxetine blockade of I_{HERG}

Measurements of I_{HERG} blockade by fluoxetine, an SSRI with a fatal toxicity index 50-fold lower than imipramine [1], were made to allow for a direct comparison of the two drugs' abilities to block I_{HERG} in a single experimental system; experiments and protocols were as per citalopram above, and the results are shown in Fig. 1B. The observed IC_{50} for fluoxetine was 1.50 μM, and the Hill coefficient was 0.79 ($n = 4$–9 for all concentrations); again this Hill coefficient may suggest that there was a one-to-one interaction between drug molecule and channel. This observed IC_{50} for fluoxetine in our system is similar to that reported recently (1.0 μM) in abstract form, where the experimenters used CHO cells transfected with HERG [23]. Our data suggest that fluoxetine is a slightly more potent blocker of I_{HERG} than is citalopram; the difference in the block potency between fluoxetine and citalopram was statistically significant (unpaired t-test, $P < 0.01$ and $P < 0.05$ at 1 and 10 μM of the drugs, respectively, $n = 5$–8).

3.3. Voltage effects on citalopram blockade of I_{HERG}

In order to characterise further the mechanism of citalopram's blockade of I_{HERG}, individual cells were subjected to a series of voltage commands in which the test pulse voltage (lasting 2 s) varied between −50 mV and +30 mV in increments of 10 mV, and after each test potential the tail current was observed at −40 mV. This protocol was then repeated in the presence of 10 μM citalopram. Data from a representative experiment are shown in Fig. 1C,D. The maximum tail current was plotted for each voltage (shown in Fig. 1E for the same cell as in Fig. 1C,D), and then the percentage of HERG tail current blocked by 10 μM citalopram was calculated for each cell at each voltage, and the mean for each voltage was plotted in Fig. 1F. Some voltage dependence of block was detected at voltages below 0 mV, which may be indicative of open-state dependence of block, although the trend towards voltage dependence did not attain statistical significance (analysis of variance (ANOVA), between groups, $F(7,37) = 1.96$, $P = 0.087$).

3.4. Time course of blockade

It has been shown previously that methanesulphonanilides (e.g. MK-499, E-4031) are associated with an open-state-dependent blockade of HERG (e.g. [24]), and this manifests itself during long pulse protocols with increasing blockade observed over the course of seconds [20]. An example of the blockade by 1 μM E-4031 over time during a 10 s voltage step to 0 mV is shown in Fig. 2A. By comparison, the time course of blockade by citalopram during a long pulse does not demonstrate the same kind of time dependence. Current traces for a typical experiment are shown in Fig. 2B. A mean of the ratios of current in the presence and absence of citalopram (Fig. 2C) suggests that the block showed statistically significant time dependence early during an applied depolarisation (ANOVA, $F(9,465) = 2.45$, $P = 0.01$). However, mean data plotted between 1 and 10 s (Fig. 2D) showed no significant difference in level of blockade after approximately the first second (ANOVA, $F(9,40) = 0.26$, $P = 0.98$). These data are consistent with an activation-dependent blockade of I_{HERG} by citalopram, but that this occurred with dramatically different kinetics from that commonly associated with methanesulphonanilides.

3.5. Effects of citalopram on $I_{Ca,L}$

It is known that effects of inhibition of rapid delayed rectifier K^+ current can be offset by concomitant drug effects on opposing, inwardly directed current – in particular $I_{Ca,L}$ [25,26]. We hypothesised, therefore, that in addition to affecting I_{HERG}, citalopram might also modulate cardiac $I_{Ca,L}$. Therefore, the effects of citalopram on $I_{Ca,L}$ were investigated, by measuring $I_{Ca,L}$ from guinea pig isolated ventricular myocytes (see Section 2), and by using similar voltage clamp protocols to those employed recently by Hobai et al. [27].

Fig. 3A shows the effect of 100 μM citalopram on peak $I_{Ca,L}$ elicited by a test pulse to +10 mV. In each of seven cells, application of this concentration of citalopram led to a decrease in $I_{Ca,L}$ amplitude, with a mean percentage inhibition of 64.95 ± 2.34%. In order to ascertain whether or not this alteration in amplitude was accompanied by a change in time course of $I_{Ca,L}$ during sustained depolarisation, the time course of the current was fitted to a biexponential decline:

$$I_{Ca,L}(t) = A_1 \exp(-t/\tau_1) + A_2 \exp(-t/\tau_2) + C \quad (1)$$

where A_1 and A_2, and τ_1 and τ_2 are the maximal amplitudes and time constants of the two exponentials, respectively, C is any residual current component and t is time. The effects of citalopram on the fast and slow time constants of inactivation are shown in Fig. 3B. Neither time constant was significantly affected by citalopram ($P > 0.1$; $n = 7$ cells). Thus, citalopram reduced $I_{Ca,L}$ amplitude without significantly affecting the inactivation time course of the current.

Inhibition of $I_{Ca,L}$ by citalopram was concentration-dependent. The effects of citalopram concentrations between 1 and 100 μM were tested, and the resulting mean (± S.E.M.) fractional inhibition values were plotted against concentration as shown in Fig. 3C. The inhibitory action of citalopram against $I_{Ca,L}$ was less potent than that against I_{HERG} (cf. Fig. 3A with Fig. 1B).

The characteristics of inhibition by citalopram of $I_{Ca,L}$ were examined further by studying the drug's action on $I_{Ca,L}$ elicited at different test voltages between −40 and +50 mV. Fig. 4A shows that 100 μM citalopram inhibited $I_{Ca,L}$ across the range of test potentials. In order to determine the effects of the agent on the voltage-dependent activation parameters for $I_{Ca,L}$, the $I_{Ca,L}$–V relations in control and drug were fitted by a modified Boltzmann relation:

$$I_{Ca,L} = G_{max}(V_m - V_{rev})/\{1 + \exp[(V_{0.5} - V_m)/k]\} \quad (2)$$

where $V_{0.5}$ and k are the half maximal activation membrane potential and the slope of the curve, respectively, G_{max} is maximal $I_{Ca,L}$ conductance and V_{rev} is the reversal potential for $I_{Ca,L}$ extrapolated from the linear portion of the ascending limb of the I–V relation. Values for $V_{0.5}$ in control and

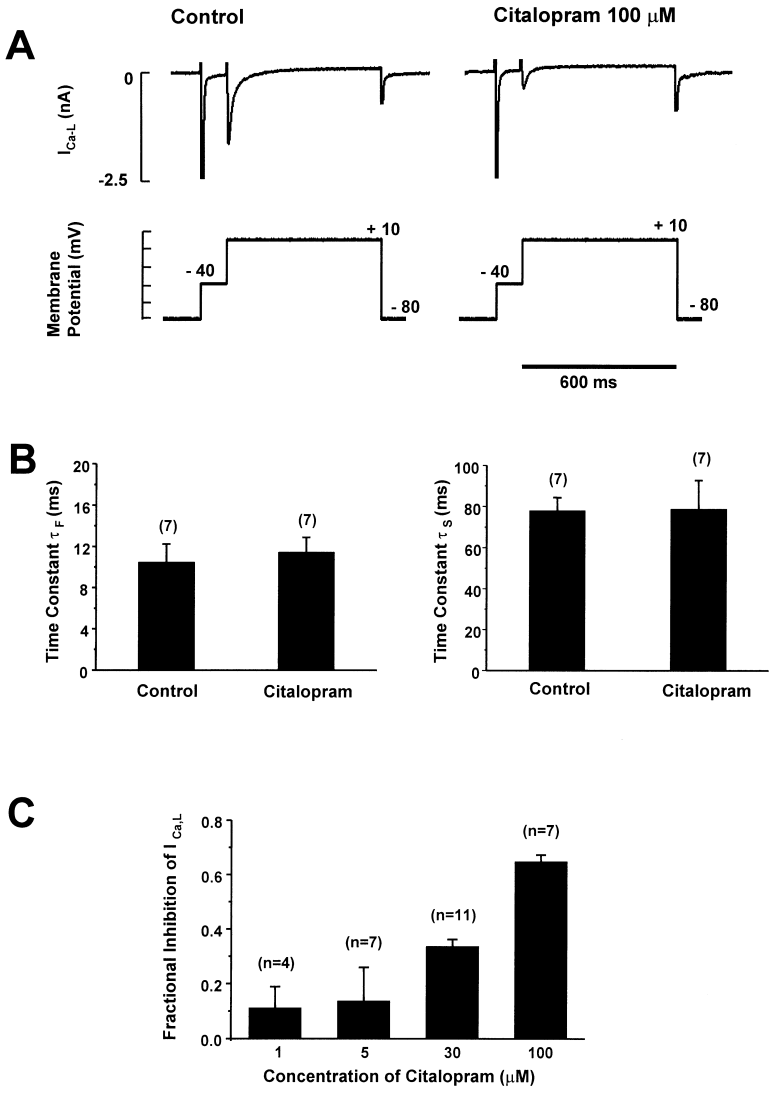

Fig. 3. Citalopram inhibits ventricular $I_{Ca,L}$. A: Upper traces show representative ionic currents elicited by the voltage protocol illustrated in the lower traces. After a pre-pulse to −40 mV, a test pulse to +10 mV elicited $I_{Ca,L}$. The amplitude of $I_{Ca,L}$ in the presence of 100 μM citalopram (right panel) was reduced compared to that in control (left panel). Bar charts (B) show effects of citalopram on the magnitudes of fast (τ_f – left panel) and slow (τ_s – right panel) time constants of inactivation of $I_{Ca,L}$ determined using Eq. 2 (see text). Neither time constant was significantly altered by citalopram. In (C) the bar chart shows the concentration dependence of $I_{Ca,L}$ inhibition (shown as 'fractional inhibition') between 1 and 100 μM citalopram.

citalopram from each of six cells were pooled, in order to determine and compare mean ± S.E.M. parameters. In control, $V_{0.5}$ and k were −10.95 ± 1.91 mV and 6.01 ± 0.19 mV, respectively; whilst in citalopram the $V_{0.5}$ mean k values were −12.80 ± 1.19 mV and 6.21 ± 0.29 mV, respectively. Neither $V_{0.5}$ nor k was statistically significantly altered by citalopram ($P > 0.2$ in each case).

The effect of citalopram on the voltage dependence of inactivation of $I_{Ca,L}$ was determined using the protocol shown in Fig. 4B (inset). An initial pulse elicited an $I_{Ca,L}$ current; this was followed by conditioning pulses to a range of voltages, in order to produce different levels of $I_{Ca,L}$ inactivation. The conditioning pulses were then followed by a test pulse to +10 mV. $I_{Ca,L}$ during the test pulse following conditioning pulses to differing potentials was expressed as a proportion of the maximal $I_{Ca,L}$ value obtained, and plotted against the corresponding conditioning voltage. The resulting plots for each of eight cells were fitted by a Boltzmann function:

$$I_{Ca,L}/I_{Ca,L(max)} = 1-1/\{1+\exp[(V_{0.5}-V_m)/k]\} \quad (3)$$

where $I_{Ca,L(max)}$ is maximum $I_{Ca,L}$. By pooling values for both $V_{0.5}$ and k for both control solution and in 100 μM citalopram, the mean values for control $V_{0.5}$ and k were found to be: −26.97 ± 1.43 mV and 4.09 ± 0.08 mV, respectively. In the presence of citalopram $V_{0.5}$ and k were −52.71 ± 2.40 mV and 8.22 ± 0.50 mV, respectively. The alterations to both $V_{0.5}$ and k values were significant ($P < 0.001$).

Arrhythmias arising from HERG channel blockade are believed to correlate at the cellular level with early afterdepolarisations (EADs), events that arise due to increased Ca^{2+} entry as the membrane potential scans the $I_{Ca,L}$ 'window' during

action potential repolarisation [28,29]. Using $V_{0.5}$ and k values obtained from the I–V fits (Fig. 4A) and inactivation curve plots (Fig. 4B), we were able to simulate the effects of citalopram on the $I_{Ca,L}$ 'window', as follows: the inactivation parameters were simulated at 2 mV intervals between −100 mV and +20 mV using Eq. 3, and activation parameters were simulated using the equation:

$$\text{Activation variable} = 1/(1+\exp[(V_{0.5}-V_m)/k]) \quad (4)$$

where 'activation variable' at any test potential V_m occurs within the range 0–1; $V_{0.5}$ and k have similar meanings to those in Eq. 2. For both conditions, the area of overlap of activation and inactivation curves in Fig. 4C denotes the $I_{Ca,L}$ window region – a potential range over which a small persistent Ca^{2+} entry would be anticipated. Thus, in the simulated presence of citalopram, the $I_{Ca,L}$ 'window' was both smaller than that in control, and was shifted towards more negative potentials – both effects likely attributable to the alterations in voltage-dependent inactivation kinetics of the current.

Collectively, our findings regarding $I_{Ca,L}$ are indicative of a direct interaction between citalopram with the $I_{Ca,L}$ channel

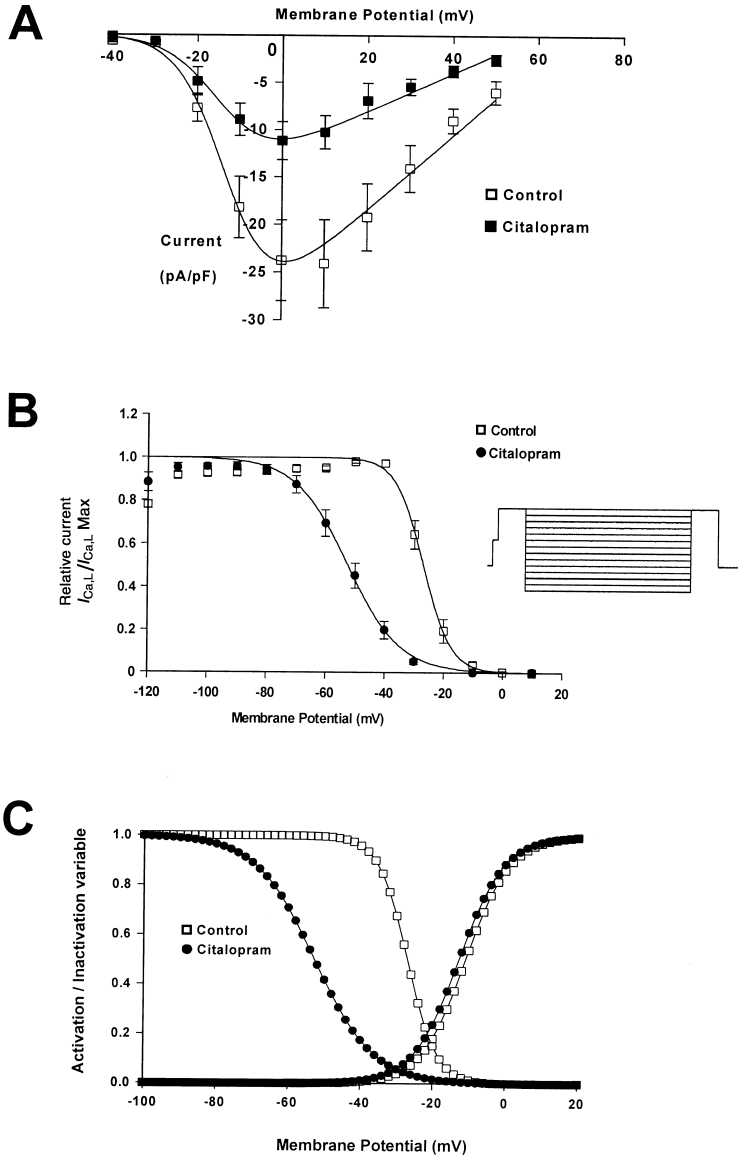

Fig. 4. Effect of citalopram on voltage-dependent properties of $I_{Ca,L}$. A: Current–voltage (I–V) relations for $I_{Ca,L}$ in control and 100 μM citalopram. $I_{Ca,L}$ density (pA/pF) values were obtained at potentials between −40 and +50 mV, and were pooled to produce mean values from six cells. For each condition, the mean data were fitted by a modified Boltzmann equation (control: $V_{0.5} = -12.56$ mV, $k = 5.58$ mV; citalopram: $V_{0.5} = -13.92$, $k = 6.20$ mV). B: Plots of steady-state inactivation curves for $I_{Ca,L}$ in control and in 100 μM citalopram. Voltage protocol shown in inset. Data from each of eight cells were pooled, to give mean ± S.E.M. values for the inactivation variable at each potential. The plots in control and drug were fitted by Eq. 3 (see Section 3). Control: $V_{0.5} = -26.90$ mV, $k = 4.74$ mV; citalopram: $V_{0.5} = -52.45$, $k = 8.94$ mV. C: $I_{Ca,L}$ 'window', simulated for control and citalopram. Activation parameters were simulated at 2 mV intervals between −100 and +20 mV, using Eq. 4. The mean $V_{0.5}$ and k values obtained by pooling the values obtained from fits to individual cells were used (control: −10.95 mV and 6.01 mV, for $V_{0.5}$ and k, respectively; citalopram: −12.80 mV and 6.21 mV for $V_{0.5}$ and k, respectively). Inactivation parameters were also simulated at 2 mV intervals on the basis of parameters derived from pooling $V_{0.5}$ and k values for individual cells (control: −26.97 mV and 4.09 mV for $V_{0.5}$ and k, respectively; citalopram: −52.71 mV and 8.22 mV, respectively). For each condition, the area of overlap of the activation and inactivation curves denotes the $I_{Ca,L}$ window.

that (a) resulted in decreased flow of $I_{Ca,L}$ across a range of test potentials, (b) altered voltage-dependent inactivation kinetics, without an altered inactivation time course of the current (c) would have decreased steady-state Ca^{2+} entry over the range of window voltages. Previous data for $I_{Ca,L}$ block by the SSRI fluoxetine using conventional microelectrodes and whole-cell patch clamp of guinea pig and rabbit papillary muscles and single canine ventricular myocytes are consistent with conclusions (a) and (b) [30], although they did not directly investigate 'window' $I_{Ca,L}$.

4. Discussion

The foregoing data indicate that I_{HERG} is sensitive to inhibition by citalopram. In our heterologous mammalian system the potency of citalopram's block is similar to that of imipramine and amitriptyline [16], but the potency of fluoxetine is stronger than that of all three other antidepressants. The mechanism of block by citalopram can be distinguished from that of E-4031 with a long pulse protocol, in that substantially less current is blocked initially by E-4031 when the first depolarising pulse in the presence of drug is applied, even though the percentage block that develops later in 1 μM E-4031 far exceeds the block by 10 μM citalopram. Using a similar protocol, the mechanism of imipramine can be distinguished from that of citalopram in that the imipramine block appears in part almost immediately, and may have a component of closed-state block [16].

In cardiomyocytes, the block by citalopram of native currents mediated by HERG would reduce net repolarising current. In turn, this would be expected to result in ventricular action potential prolongation, and thereby would lead to prolongation of the QT interval of the ECG and the associated risk of *Torsades de pointes* [31]. However, the reported safety profile for citalopram [7,8] has not been suggestive of this as a major risk factor in citalopram use. This is consistent with the existence of an additional drug action, affecting a depolarising current that modulates the action potential plateau duration, such as $I_{Ca,L}$.

After commencement of citalopram treatment, in 277 patients with pre-existing heart disease or on drug therapy with agents known to have the potential for QT_c prolongation, no further prolongation of QT_c was detected [9]. By contrast to the situation at therapeutic dosages, in Sweden a forensic analysis of six suicides concluded that suicidal citalopram overdose was associated with the deaths, and no other modes of death could be found by forensic investigation [11]. Another report of five citalopram-mediated attempted suicides in Sweden showed that all patients had a prolonged QT interval [12]. However, the Swedish Poisons Information Centre analysed 108 cases of acute citalopram overdose and concluded that most cases have an uneventful course and that clinically significant arrhythmias are rare [13]. Since that time, citalopram has been released in the USA, and the low incidence of reported abnormalities might result either from the fact that drug has not been released for as long as have TCAs, or from channel effects that offset the I_{HERG} blockade. An example of the latter situation is verapamil, a calcium channel blocker that blocks HERG at submicromolar concentrations [32] but is not associated with QT prolongation [25,26].

It is difficult to predict from in vitro experiments the dominant effect of a drug on arrhythmogenic risk in vivo. Despite citalopram mediating a more potent block of I_{HERG} than of $I_{Ca,L}$, the overall effect may depend on the relative contributions of the two currents to the ventricular action potential profile at particular rates. Intriguingly, in conventional microelectrode experiments on guinea pig papillary muscle, citalopram has been shown to cause a shortening, rather than a lengthening, of action potential duration [33]. The effect of citalopram on $I_{Ca,L}$ may be sufficient to either offset the QT prolongation associated with I_{HERG} blockade, or even if modest it may be sufficient to minimise the likelihood of EAD generation that would contribute to arrhythmogenesis [34,28]. As shown in Fig. 4, the $I_{Ca,L}$ window in these experiments is (a) smaller and (b) leftward-shifted in citalopram compared to control. Thus, citalopram (i) decreases $I_{Ca,L}$ amplitude, which might offset to an extent QT prolongation and (ii) produces a smaller window and at more negative potentials – these effects may reduce the likelihood of EADs through $I_{Ca,L}$ reactivation, even if QT prolongation were to occur.

Acknowledgements: We gratefully acknowledge Mike Sanguinetti and Mark Keating for provision of the original HERG cDNA, British Biotech for provision of the pGW1H vector, Jeremy Tavare for the provision of the GFP in pCMX plasmid, Craig January for provision of the HERG-expressing HEK 293 cell line, Fabio Mammano for hosting some of these experiments including provision of resources and instruction as to the use of the Trieste rig, David Nutt for the original idea, the British Heart Foundation (Project Grants PG/2000123, PG/98081 and PG/1998028) for funding, the Wellcome Trust for funding (J.C.H.), Lesley Arberry for help with ventricular myocyte isolation, and Andy Cato for overall suggestions.

References

[1] Henry, J.A., Alexander, C.A. and Sener, E.K. (1995) Br. Med. J. 310, 221–224.
[2] Henry, J.A. (1997) Drug Saf. 16, 374–390.
[3] Freeman, J.W., Mundy, G.R., Beattie, R.R. and Ryan, C. (1969) Br. Med. J. 2, 610–611.
[4] Sacks, M.H., Bonforte, R.J., Laser, R.P. and Dimich, I. (1968) J. Am. Med. Assoc. 205, 588–590.
[5] Reilly, J.G., Ayis, S.A., Ferrier, I.N., Jones, S.J. and Thomas, S.H. (2000) Lancet 355, 1048–1052.
[6] Roose, S.P. and Spatz, E. (1999) J. Clin. Psychiatry 60 (Suppl. 20), 34–37.
[7] Keller, M.B. (2000) J. Clin. Psychiatry 61, 896–908.
[8] Parker, N.G. and Brown, C.S. (2000) Ann. Pharmacother. 34, 761–771.
[9] Muldoon, C.G. (1995) Citalopram: Monitoring the QT_c Interval, Report #3, Lundbeck, Copenhagen.
[10] Enemark, B. (1993) Nord J. Psychiatry 47 (Suppl. 30), 57–65.
[11] Öström, M., Eriksson, A., Thorson, J. and Spigset, O. (1996) Lancet 348, 339–340.
[12] Grundemar, L., Wohlfart, B., Lagerstedt, C., Bengtsson, F. and Eklundh, G. (1997) Lancet 349, 1602.
[13] Personne, M., Persson, H. and Sjöberg, E. (1997) Lancet 350, 518–519.
[14] Valenzuela, C., Sanchez-Chapula, J., Delpon, E., Elizalde, A., Perez, O. and Tamargo, J. (1994) Circ. Res. 74, 687–699.
[15] Witchel, H.J. and Hancox, J.C. (2000) Clin. Exp. Pharm. Physiol. 27, 753–766.
[16] Teschemacher, A.G., Seward, E.P., Hancox, J.C. and Witchel, H.J. (1999) Br. J. Pharmacol. 128, 479–485.
[17] Jo, S.H., Youm, J.B., Lee, C.O., Earm, Y.E. and Ho, W.K. (2000) Br. J. Pharmacol. 129, 1474–1480.
[18] Tie, H., Walker, B.D., Valenzuela, S.M., Breit, S.N. and Campbell, T.J. (2000) Lancet 355, 1825.
[19] Hancox, J.C., Levi, A.J. and Witchel, H.J. (1998) Pflüg. Arch. 436, 843–853.

[20] Zhou, Z., Gong, Q., Ye, B., Makielski, J.C., Robertson, G.A. and January, C.T. (1998) Biophys. J. 74, 230–241.
[21] Levi, A.J. and Issberner, J. (1996) J. Physiol. (Lond.) 493, 19–37.
[22] Lagostena, L., Ashmore, J.F., Kachar, B. and Mammano, F. (2001) J. Physiol. 531, 693–706.
[23] Trube, G. and Pflimlin, P. (2001) Inhibition of the HERG-mediated K^+ current by fluoxetine. Channelopathies 2001: An international meeting on ion channels and their relation to human disease.
[24] Spector, P.S., Curran, M.E., Keating, M.T. and Sanguinetti, M.C. (1996) Circ. Res. 78, 499–503.
[25] Bril, A., Gout, B., Bonhomme, M., Landais, L., Faivre, J.F., Linee, P., Poyser, R.H. and Ruffolo, R.R.J. (1996) J. Pharmacol. Exp. Ther. 276, 637–646.
[26] Bril, A., Forest, M.C., Cheval, B. and Faivre, J.F. (1998) Cardiovasc. Res. 37, 130–140.
[27] Hobai, I.A., Hancox, J.C. and Levi, A.J. (2000) Am. J. Physiol. Heart Circ. Physiol. 279, H692–H701.
[28] January, C.T. and Riddle, J.M. (1989) Circ. Res. 64, 977–990.
[29] Makielski, J.C. and January, C.T. (1998) Card. Electrophysiol. Rev. 2, 132–135.
[30] Pacher, P., Magyar, J., Szigligeti, P., Banyasz, T., Pankucsi, C., Korom, Z., Ungvari, Z., Kecskemeti, V. and Nanasi, P.P. (2000) Naunyn Schmiedebergs Arch. Pharmacol. 361, 67–73.
[31] Sanguinetti, M.C. and Keating, M.T. (1997) News Physiol. Sci. 12, 152–157.
[32] Chouabe, C., Drici, M.D., Romey, G., Barhanin, J. and Lazdunski, M. (1998) Mol. Pharmacol. 54, 695–703.
[33] Pacher, P., Bagi, Z., Lako-Futo, Z., Ungvari, Z., Nanasi, P.P. and Kecskemeti, V. (2000) Gen. Pharmacol. 34, 17–23.
[34] January, C.T. and Moscucci, A. (1992) Ann. N.Y. Acad. Sci. 644, 23–32.